Applied Catalysis B: Environmental 129 (2013) 273–281

Contents lists available at SciVerse ScienceDirect

Applied Catalysis B: Environmental

journal homepage: www.elsevier.com/locate/apcatb

Review

Platinum oxide formation and reduction during NO oxidation on a diesel oxidation catalyst—Macrokinetic simulation

K. Hauff*, H. Dubbe, U. Tuttlies, G. Eigenberger, U. Nieken[1]

Institute of Chemical Process Engineering, University Stuttgart, Boeblinger Str. 78, 70199 Stuttgart, Germany

ARTICLE INFO

Article history:
Received 20 June 2012
Received in revised form 7 September 2012
Accepted 13 September 2012
Available online 26 September 2012

Keywords:
NO oxidation
Platinum oxidation
Deactivation
Macrokinetic model
Inverse hysteresis

ABSTRACT

The activity of a diesel oxidation catalyst (Pt-γ-Al_2O_3) is strongly influenced by the reaction conditions due to platinum oxidation, which drastically decreases the NO oxidation activity. Reactivation is possible with normal exhaust gas since platinum oxide can be reduced by NO in an atmosphere with high oxygen content at temperatures below 200 °C. A macrokinetic model is presented which takes into account the deactivation due to platinum oxidation. A standard model is extended by an additional balance of the platinum fraction and by reactions for platinum oxide formation ($Pt + 0.5\ O_2 \rightleftharpoons PtO$) and reduction ($PtO + NO \rightarrow Pt + 0.5\ NO_2$). It is assumed (1) that platinum oxide is not inactive but has a lower activity, (2) that small amounts of NO_2 have no impact on the oxidation in the presence of high oxygen concentrations and (3) that formation of PtO_2 is negligible and that PtO is the main platinum oxide species formed. The NO oxidation rate is calculated for highly active sites (platinum) and sites with lower activity (platinum oxide). The actual reaction rate is calculated as a function of the platinum oxide fraction. With this extended macrokinetic model a good prediction of NO conversion is achieved. For model calibration and validation, isothermal experiments with either constant temperature or linear temperature ramps are employed. The model can be transferred to catalysts with lower platinum loading or aged catalysts, if only the NO oxidation on platinum and platinum oxide is reparameterised.

Contents

1. Introduction

The diesel oxidation catalyst (DOC) is nowadays often combined with a diesel particulate filter (DPF) and either a NO_x storage catalyst (NSC) or a selective catalytic reduction (SCR) catalyst. In this configuration the task of the DOC is to increase the NO_2/NO_x ratio which is improving the performance of the downstream units [1]. Therefore a high NO oxidation activity has to be maintained.

Several investigations revealed that the DOC activity changes during the NO oxidation. A deactivation over time is observed [2–5], for example the NO conversion decreased from 76 to 25% on a Pt/Al_2O_3-DOC with 110 gPt/ft^3 at 300 °C within 3 h [6]. The deactivation is caused by the formation of platinum oxide, which is less active for the oxidation of NO compared to platinum [7], because the binding ability of oxide towards O, O_2 and NO is weaker and the reaction barriers change [8,9]. X-ray absorption spectroscopy and in situ XANES experiments revealed that platinum oxidises with increasing time on stream during NO oxidation depending on platinum particle size [10]. A slow oxidation of the particle surface takes place, which might cause surface rearrangements but no formation of bulk oxides. Pt is in a metastable state between Pt with reactive chemisorbed (surface-bound) oxygen and platinum oxides, which

* Corresponding author. Tel.: +49 711 685 85245; fax: +49 711 685 85242.
E-mail addresses: karinhauff@web.de (K. Hauff), ulrich.nieken@icvt.uni-stuttgart.de (U. Nieken).
[1] Tel.: +49 711 685 85229; fax: +49 711 685 85242.

0926-3373/$ – see front matter © 2012 Elsevier B.V. All rights reserved.
http://dx.doi.org/10.1016/j.apcatb.2012.09.022

List of symbols

a_i^j	exponent of the mole fraction in the inhibition term
a_{geo}	specific geometric surface (m^2/m^3)
D_{bulk}	diffusion coefficient in the gas bulk (m^2/s)
E_a	activation energy (J/(mol K))
K_{NO,O_2}	equilibrium constant of NO oxidation
K_{Pt,O_2}	equilibrium constant of Pt oxidation
k_i	reaction rate constant of reaction i (mol/m^2 s)
K_i^{inhj}	inhibition term constant of component j in reaction i
I_i	inhibition term of reaction i
p	pressure (Pa)
q_i^j	exponent of the mole fraction
r_i	reaction rate of reaction i (mol/m^2 s)
T	temperature (K)
v^b	bulk velocity (m/s)
y_j^b	mole fraction of component j in the bulk
y_j^s	mole fraction of component j at the surface
ϵ_b	open frontal area
θ_{Pt}	fraction of platinum
θ_{PtO}	fraction of platinum oxide
$\nu_{i,j}$	stoichiometric coefficient
ρ_{Pt}	platinum density (mol Pt/m^2)

are assumed to be inactive. On the contrary, Wang [8] calculated by DFT that PtO_2 is not inactive but has a lower activity than metallic Pt. Two possible oxidation agents exist in the typical diesel exhaust gas: O_2 and NO_2. Hauptmann [5] assumes that the formation of platinum oxide is mainly induced by NO_2 due to its ability to generate a higher oxygen surface coverage than O_2 because of its coordinative flexibility [11–13].

The deactivation by platinum oxidation is reversible. Platinum oxide decomposes above 400 °C in UHV [14] and above 650 °C in ambient pressure [9]. Alternatively, platinum oxide can be reduced at lower temperatures by NH_3 or NO [9]. Interestingly, Hauptmann found that NO is able to reduce platinum oxide even in a net oxidising atmosphere with 450 ppm NO in 6% O_2 [5]. When the gas atmosphere is kept constant and the temperature is linearly increased and decreased between 80 and 370 °C, platinum oxide formation and reduction depends only on the temperature und the thereby induced changes of NO/NO_2-ratio under oxygen excess. The actual activity of the catalyst therefore strongly depends on the pretreatment and the operating conditions.

Comprehensive measurements by the authors have already been published in [15] for a 130.06 g Pt/ft^3-γ-Al_2O_3 DOC. The measurements were performed in an isothermal flat bed reactor to avoid temperature gradients. For the example shown in Figs. 1 and 2, the catalyst was pretreated with 3% H_2 at 350 °C for 1800 s and afterwards cooled down in inert atmosphere to 160 °C. The feed was kept constant with 500 ppm NO, 12% O_2 and 10% H_2O in nitrogen while the temperature was increased to 400 °C and subsequently cooled down to 160 °C with a linear ramp of 5 K/min. A repetition of the temperature cycle followed immediately.

The first run of the temperature cycle is shown in Fig. 1. In the beginning (run 1a), the highest NO oxidation activity can be observed due to the reductive pretreatment. Platinum oxide is progressively formed in the oxidising atmosphere. By different experiments, it was shown that platinum oxide decomposes at higher temperatures (>350 °C) [15]. Thermal decomposition of platinum oxide was also reported in literature but at higher temperatures (above 530 °C) and for much smaller platinum particles of about 2 nm diameter [16]. A reoxidation of the platinum takes place

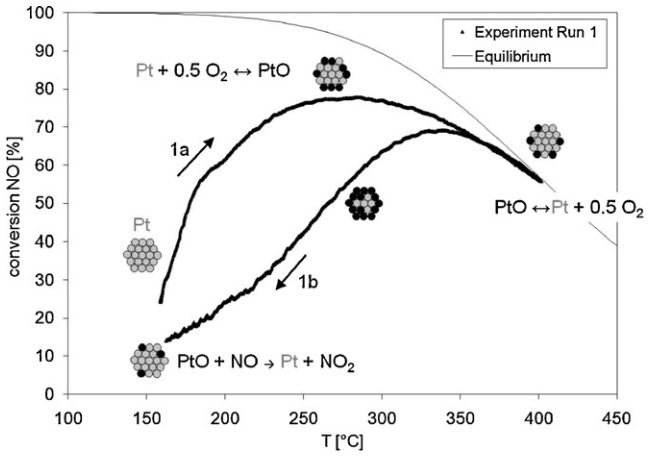

Fig. 1. First run of NO oxidation (500 ppm NO, 12% O_2, 10% H_2O) directly after reducing pretreatment with 3% H_2 with linear temperature ramp (±5 K/min). (1a) Heating, (1b) cooling, *Equilibrium* refers to the maximum possible NO conversion due to the thermodynamical limitation of $NO + \frac{1}{2}\ O_2 \rightleftharpoons NO_2$.

while cooling down (run 1b). Interestingly NO is able to reduce platinum oxide in a net oxidising atmosphere at low temperatures, where NO oxidation is slow. This causes a partial reactivation of the catalyst. Thus the second ramp with increasing temperature (2a, see Fig. 2) has a higher NO conversion than the cooling ramps (1b + 2b). The second cooling temperature ramp (2b) is identical with the first cooling ramp (1b). Hence, the Light-Out of NO oxidation takes place at a higher temperature than the Light-Off, which is contrary to the well known ignition/extinction hysteresis of CO oxidation and therefore called an inverse hysteresis by Hauptmann [5].

Several further experiments have been accomplished by the authors to elucidate the conditions of formation and decomposition of platinum oxide [15]. The employed types of experiments are:

1. Linear temperature ramp between 160 and 400 °C (Fig. 3 in [15]).
2. Variation of minimal temperature (160, 180 and 200 °C) of the ramp (Fig. 6 in [15]).
3. Temperature ramp with holding at 160, 180 or 200 °C for 30 min in different gas atmospheres (Fig. 6 in [15]).
4. Cooling down in nitrogen (Fig. 5 in [15]).

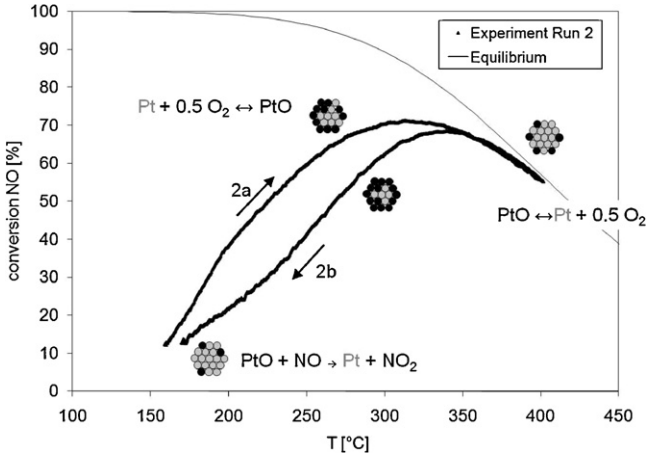

Fig. 2. Second run of NO oxidation (500 ppm NO, 12% O_2, 10% H_2O) directly after the first run without any further pretreatment with linear temperature ramp (±5 K/min). (2a) Heating, (2b) cooling, *Equilibrium* refers to the maximum possible NO conversion due to the thermodynamical limitation of $NO + \frac{1}{2}\ O_2 \rightleftharpoons NO_2$.

5. Temporal progress of deactivation at constant temperature and feed composition (Fig. 7 in [15]).

The experiments proved that the deactivation by platinum oxidation is a very slow process. Therefore, a steady state is not reached during the temperature ramp experiments. Reduction of PtO by NO is possible in an oxygen-rich atmosphere (500 ppm NO, 12% O_2, 10% H_2O) below 220 °C. At temperatures above 300 °C, platinum oxide is decomposed to platinum due to thermal decay. Small NO_2 concentrations (<200 ppm) have no influence on the progress of platinum oxidation in the presence of 12% O_2 as experiments with and without NO_2 in the feed have shown. Platinum oxidation is mainly driven by high O_2 concentrations, which is also supported by an observed deactivation of CO oxidation under lean conditions in the absence of NO_x. A qualitative confirmation of progressive platinum oxide formation with increasing duration of NO oxidation is achieved by H_2-titration (Fig. 13 in [15]).

The de- and reactivation of the catalyst by platinum oxide formation and reduction has to be taken into account in the model for a correct prediction of the conversion. Hauptmann [5] introduced a microkinetic model with a platinum oxidation mechanism. The formed platinum oxide is assumed to be inactive, by which the number of available surface sites for catalytic conversion is reduced. The model is able to reproduce the NO conversion for an experiment with linear temperature ramps between 80 and 370 °C is reproduced very well.

In this contribution, a macrokinetic model is developed and validated for describing deactivation by platinum oxidation. Macrokinetics consider only the rate determining reaction steps in a global reaction rate approach instead of detailing into separate single ad-, desorption and surface reaction steps. The advantage of macrokinetic models is the substantially reduced number of adjustable rate parameters and the decreased computational effort. It is therefore the typical model type used in automotive industry.

In macrokinetic modelling, the activity of catalysts with different precious metal loadings can also be considered by including the catalytic surface area as an independent variable in the reaction rate term [17–19]. It was shown that this approach can be applied as well for irreversible catalyst deactivation due to thermal aging [20,21], which causes sintering of the precious metal particles.

In this paper, a macrokinetic model reproducing the reversible deactivation by platinum oxidation is developed. The model is validated by comparison with several isothermal conversion measurements under different types of transient conditions as well as under constant feed and temperature. To keep the model manageable, the number of additional parameters is kept as low as possible in order to avoid parametric multiplicity.

2. Simulation

2.1. Reactions

Focussing on NO conversion in typical lean diesel exhaust gas, O_2, NO and NO_2 shall be considered as reactants while H_2O, CO_2 and N_2 can be considered constant due their high excess. Pt, PtO and PtO_2 have been detected by XPS on a similar catalyst (Pt/Al_2O_3-DOC) after pretreatment with a nearly identical gas atmosphere [6]. Taking these species into account, the following set of pseudo macrokinetic reactions Eqs. (1)–(4) are suggested to describe platinum oxidation in a macrokinetic model:

$$Pt + 0.5\ O_2 \rightleftharpoons PtO \quad (1)$$

$$PtO + 0.5\ O_2 \rightleftharpoons PtO_2 \quad (2)$$

$$Pt + NO_2 \rightleftharpoons PtO + NO \quad (3)$$

$$PtO + NO_2 \rightleftharpoons PtO_2 + NO \quad (4)$$

From the experiments described in [15], it can be concluded that:

- Above 350 °C, platinum oxide decomposes to platinum due to thermal decay. Therefore, reactions (1) and (2) are given as equilibrium reactions.
- Platinum oxide can be reduced by NO at low temperatures. Hence, reactions (3) and (4) are reversible.
- As there is no indication that a distinction between PtO and PtO_2 is necessary, only PtO is used in the model. Therefore, reactions (2) and (4) are not further considered in the model. In fact, rather a certain O-atom/Pt-atom ratio will arise in the platinum particle depending on how much oxygen atoms are incorporated in the platinum crystal lattice.
- A typical diesel exhaust gas has a high oxygen content in the range of 10% and contains little NO_2 concentrations below 100 ppm. Experiments with and without NO_2 [15] proved that the NO_2 content has no influence on the progress of platinum oxidation under oxygen excess. Therefore the formation of platinum oxide by NO_2 is neglected.
- Compared to the oxidation of the pollutants, the formation and reduction of platinum oxide are very slow processes which take place over minutes and hours.
- Oxidation of platinum by O_2 and reduction of platinum oxide by NO are competing reactions. The activation energy of Eq. (1) has to be higher than of Eq. (3), because the oxidation of platinum is slower at low temperatures but is getting faster than the reduction of platinum oxide with rising temperature.

Hence, the reaction scheme can be simplified to:

$$Pt + 0.5\ O_2 \rightleftharpoons PtO \quad (5)$$

$$PtO + NO \rightarrow Pt + NO_2 \quad (6)$$

Pt stands thereby for a metallic platinum surface site. PtO is assumed to be less active and stands for oxidised platinum not for a platinum site with adsorbed, reactive oxygen like in microkinetics.

2.2. Model

In the following it will be assumed that the catalysed gas reactions take place on Pt and on PtO with different rates according to the DFT and microkinetic study of Wang [8], who observed a lower activity for PtO_2 than for metallic Pt. The conversion of the catalyst between Pt and PtO is described according to Eqs. (1) and (6) with θ_{Pt} and $\theta_{PtO} = 1 - \theta_{Pt}$ as respective fractions of sites. Unlike in microkinetic models, θ_{PtO} does not describe the surface coverage of adsorbed oxygen but the fraction of platinum atoms, which are oxidised. Adsorbates on Pt and PtO (e.g. OH groups) are not taken into account. As PtO decomposes at higher temperatures due to thermodynamic limitations, the reaction rate of Eq. (1) has to be formulated as an equilibrium reaction:

$$r_{Pt,O_2} = A_{Pt,O_2}\ \exp\left(\frac{-E_{Pt,O_2}}{\mathbf{R}}\left(\frac{1}{T} - \frac{1}{493.15\mathrm{K}}\right)\right) \cdot \left(\theta_{Pt}\ y_{O_2}^{0.5} - \frac{1}{K_{Pt,O_2}}(1-\theta_{Pt})\right) \quad (7)$$

For the reduction of PtO by NO the reverse reaction can be neglected, since the oxidation of Pt by NO_2 is negligible compared to O_2 [15], leading to

$$r_{PtO,NO} = A_{PtO,NO}\ \exp\left(\frac{-E_{PtO,NO}}{\mathbf{R}}\left(\frac{1}{T}-\frac{1}{493.15\mathrm{K}}\right)\right) \cdot \theta_{PtO}\ y_{NO} \tag{8}$$

The reaction order is assumed to equal the stoichiometry. The amount of θ_{Pt} can then be calculated for each position in the monolith by the mass balance

$$\frac{d\theta_{Pt}}{dt} = \frac{1}{\rho_{Pt}}\ (-r_{Pt,O_2} + r_{PtO,NO}). \tag{9}$$

Oxygen diffusion in the platinum particles, e.g. to subsurface regions is not taken into account.

For the conversion of the gaseous components a one-dimensional convection/diffusion model for gas phase (Eq. (10)) and solid phase (Eq. (11)) will be applied. Gaseous species are denoted by y_j^b, species at the washcoat surface by y_j^s. Both phases are connected by mass transfer terms. Sherwood number correlations are used to calculate the external mass transfer coefficients β_j. The influence of internal mass transfer resistances in the washcoat is implicitly included in the macrokinetics. The reaction rates are calculated upon Langmuir–Hinshelwood-kinetics as reported earlier [20]. Quasi steady state is assumed for the solid phase balance.

$$\frac{\partial y_j^b(x,t)}{\partial t} = -v^b\cdot\frac{\partial y_j^b(x,t)}{\partial x} + D_{bulk}\cdot\frac{\partial^2 y_j^b(x,t)}{\partial x^2} - a_{geo}\cdot\beta_j\cdot(y_j^b(x,t)-y_j^s(x,t)) \tag{10}$$

$$0 = \beta_j\cdot(y_j^b(x,t)-y_j^s(x,t)) + \frac{\mathbf{R}T}{p}\cdot\sum_{i=1}^{I^S}\nu_{i,j}\cdot r_i^s(y_j^s) \tag{11}$$

A heat balance is not taken into account due to isothermal reaction conditions. The actual gas phase velocity is assumed to change only with temperature and pressure ($v^b(T) = v^b(T_0)\cdot T/T_0\cdot p_0/p$) and not due to the reactions. The model equations have been implemented in the simulation software PREDICI [22]. The parameter estimation is accomplished by a least squares fit with a damped Gauss–Newton algorithm.

In the following, the reversible NO oxidation

$$NO + 0.5\ O_2 \rightleftharpoons NO_2 \tag{12}$$

will be considered as the only gas phase reaction. It shall proceed over Pt or over PtO with different rates as given below. The fact that small amounts of NO and NO_2 are also converted in reaction (6) will not be accounted for in the mass balance since this influence is negligible compared to reaction (12). The NO oxidation rate is calculated by Eq. (13). The equilibrium constant K_{NO,O_2} is calculated using data from NIST Chemistry WebBook [23].

$$r_{NO,O_2}^{Pt/PtO} = \frac{k^{Pt/PtO}}{\left(I_{NO,O_2}^{Pt/PtO}\right)^2}\cdot y_{NO}^s\cdot y_{O_2}^s \cdot\left(1-\frac{y_{NO_2}^s}{y_{NO}^s\sqrt{y_{O_2}^s}\cdot K_{NO,O_2}}\right)$$

$$k^{Pt/PtO}(T) = k_0^{Pt/PtO}(573.15\mathrm{K})\cdot\exp\left(-\frac{E_a}{\mathbf{R}}\left(\frac{1}{T}-\frac{1}{573.15\mathrm{K}}\right)\right) \tag{13}$$

$$I_{NO,O_2}^{Pt/PtO} = 1 + K_{NO_2}^{Inh\ Pt/PtO}\cdot y_{NO_2}^s + K_{NO}^{Inh\ Pt/PtO}\cdot y_{NO}^s$$

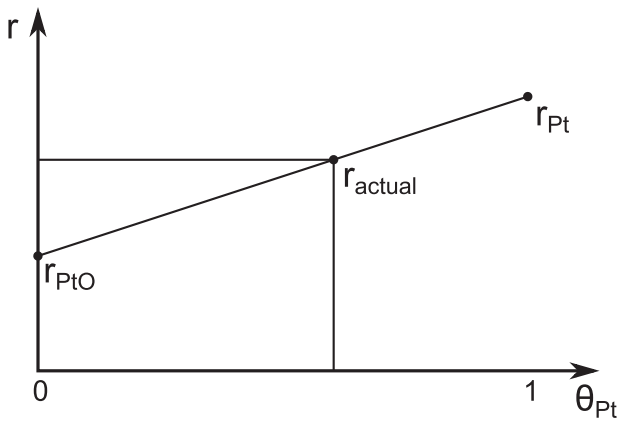

Fig. 3. Interpolation of the NO oxidation reaction rate according to the actual platinum fraction.

$$K_{NO_2}^{Inh\ Pt/PtO}(T) = K_{NO_2}^{Inh\ Pt/PtO}(573.15\mathrm{K})\cdot\exp\left(-\frac{E_{NO_2}^{Inh\ Pt/PtO}}{\mathbf{R}}\left(\frac{1}{T}-\frac{1}{573.15\mathrm{K}}\right)\right)$$

$$K_{NO}^{Inh\ Pt/PtO}(T) = K_{NO}^{Inh\ Pt/PtO}(573.15\mathrm{K})\cdot\exp\left(-\frac{E_{NO}^{Inh\ Pt/PtO}}{\mathbf{R}}\left(\frac{1}{T}-\frac{1}{573.15\mathrm{K}}\right)\right)$$

It has to be taken into account that the conversion of the NO oxidation is in turn influenced by the platinum fraction. Therefore the reaction rate of the NO oxidation has to be linked with the platinum fraction.

In the microkinetic approach of Hauptmann [5,7], the NO oxidation is assumed to run only on Pt and not on PtO. In the here presented macrokinetic model, it is assumed that platinum oxide is not inactive but has only a reduced oxidation capacity, because the binding of oxygen is weaker [9]. Therefore, two reaction rates exist: on platinum, denoted with r_{NO,O_2}^{Pt}, and on platinum oxide, named r_{NO,O_2}^{PtO}.

Both rates are calculated according to Eq. (13), but have different kinetic parameters. The actual reaction rate is then calculated in proportion to the platinum fraction θ_{Pt}, compare Fig. 3 and Eq. (14).

$$r_{NO,O_2}^{actual} = r_{NO,O_2}^{PtO} + \theta_{Pt}\cdot(r_{NO,O_2}^{Pt} - r_{NO,O_2}^{PtO}) \tag{14}$$

3. Results and discussion

3.1. Comparison with experiments for the reference catalyst

The model presented in Section 2 was fitted to the temperature ramp experiment between 160 and 400 °C shown in Figs. 1 and 2. The reaction rate designated r_{NO,O_2}^{Pt} corresponds to the maximal NO oxidation rate. The parameters (reaction rate constant, activation energy, inhibition term constant and temperature dependency) are fitted to the initial conversion of the temperature ramp experiments directly after reductive pretreatment. Alternatively, the initial conversion of the isothermal experiments presented in [15] could be used. The parameters of the minimal reaction rate r_{NO,O_2}^{PtO} are adapted to the deactivated branch of the temperature ramp between approximately 250 and 350 °C (Fig. 2, run 2b), where a high platinum oxide fraction close to 1 is assumed. Otherwise they could be fitted to the stationary, minimal conversion of each temperature step in the isothermal experiments as long as it is not limited

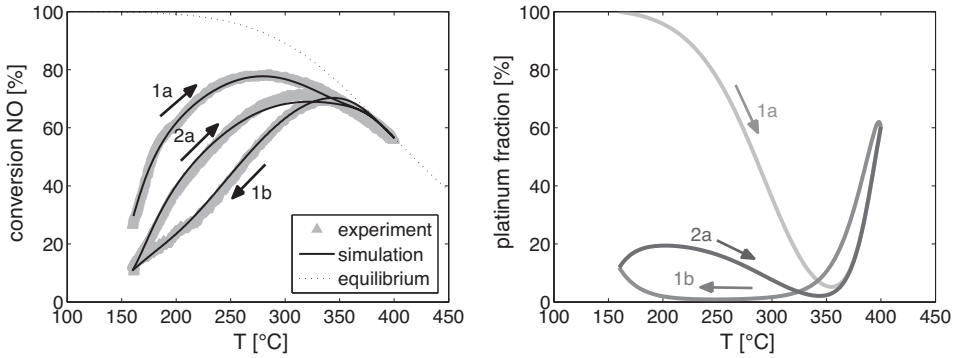

Fig. 4. Simulated conversion of NO oxidation and platinum fraction while temperature ramp between 160 and 400 °C (500 ppm NO, 12% O_2, 10% H_2O). 1a: heating, directly after reducing pretreatment with 3% H_2. 1b: subsequent cooling. 2a: second heating.

by the equilibrium of $NO + \frac{1}{2}\ O_2 \rightleftharpoons NO_2$ of $NO + \frac{1}{2}\ O_2 \rightleftharpoons NO_2$. For r^{Pt}_{NO,O_2} and r^{PtO}_{NO,O_2}, the same activation energy is used. The reaction rate constant of NO oxidation, the inhibition term constants and temperature dependencies differ (in total 5 parameters). The inhibition term parameters are affected as well possibly due to the fact that the oxidation of platinum is disordering the crystal structure of pure platinum, because oxygen atoms are placed in the crystal lattice. This will also affect ad- and desorptions. A change in the ad- and desorption ratios results in a change of the inhibition term parameters for a macrokinetic model.

The reaction rate constants (A_{Pt,O_2}, $A_{PtO,NO}$) and the activation energies (E_{Pt,O_2}, $E_{PtO,NO}$) of the platinum oxidation and platinum oxide reduction are fitted to the complete inverse hysteresis shown in Fig. 1 and 2.

The thermodynamic equilibrium parameters of $Pt + 0.5\ O_2 \rightleftharpoons PtO$ (Eq. (1)) are fitted as well. Even though thermodynamic data for bulk phase platinum oxide are available, they can not be applied, because according to literature, only a surface oxide layer is formed rather than a complete platinum oxide bulk [16,24]. In addition, the presented measurements were performed with platinum particles supported on alumina with a broad particle size distribution, compare [20]. This might cause further deviations from literature due to the reported dependency of platinum oxidation on the platinum particle size [25,26].

With the adjusted model the deactivation and reactivation during temperature cycling could be reproduced very well, see Fig. 4a.

In Fig. 4b, the calculated platinum fraction is shown for the experiment with a temperature ramp between 160 and 400 °C. According to the assumption that after the reducing pretreatment no platinum oxide exists, run 1a starts with 100% platinum. In the oxidative atmosphere with 12% O_2, the platinum fraction decreases fast. But due to the thermal decay of platinum oxide above 350 °C, the platinum fraction rises again at higher temperatures. In the subsequent cooling (run 1b), the platinum fraction decreases with decreasing temperature. It increases again for temperatures below 230 °C, because NO reduces the platinum oxide. During the subsequent second heating (run 2a), the platinum fraction increases further due to the ongoing reduction of platinum oxide. Above 250 °C, the reoxidation of the catalyst starts again, which decreases the platinum fraction until thermal decay starts at about 350 °C.

Considering the computed PtO fraction, it has to be recalled that this value is a pure model quantity, based upon the assumption that the observed minimal reaction rate r^{PtO}_{NO,O_2} corresponds to 100% platinum oxide fraction. If in future, it would be possible to measure the platinum oxide fraction independently, the model could be easily adjusted by setting the correct value of platinum oxide fraction for the minimal reaction rate r^{PtO}_{NO,O_2}.

It should be emphasised that the model was fitted to only one experiment (temperature ramp between 160 and 400 °C, Fig. 1 and 2). In total 16 parameters are related to the simulation of platinum oxide formation and reduction, see Fig. 5. These are the reaction rate constants and activation energies of Pt oxidation and PtO reduction (4 parameters), the equilibrium constant of $Pt + 0.5\ O_2 \rightleftharpoons PtO$ (Eq. (1), 1 parameter), the activation energy of NO oxidation (1 parameter) and the reaction rate constants, the inhibition term constants and temperature dependencies of NO oxidation on Pt and PtO (10 parameters).

To analyse if all 16 parameters have a significant influence on the simulation, the condition of the Fisher matrix is calculated [27]. The condition is defined as the ratio of the biggest to the smallest eigenvalue of the Fisher matrix. A value of 5.06 is obtained, which

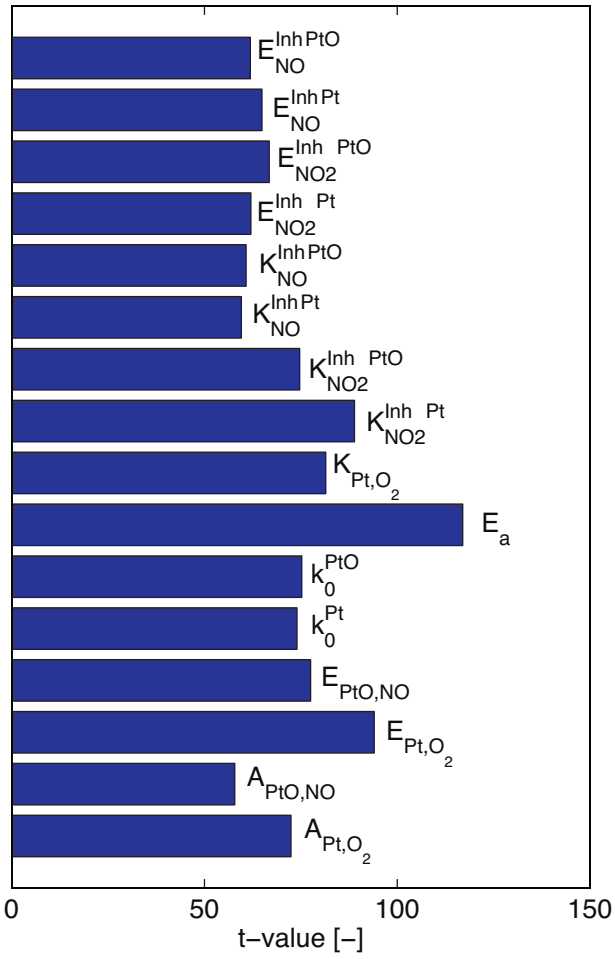

Fig. 5. *T*-values of the fitted parameters.

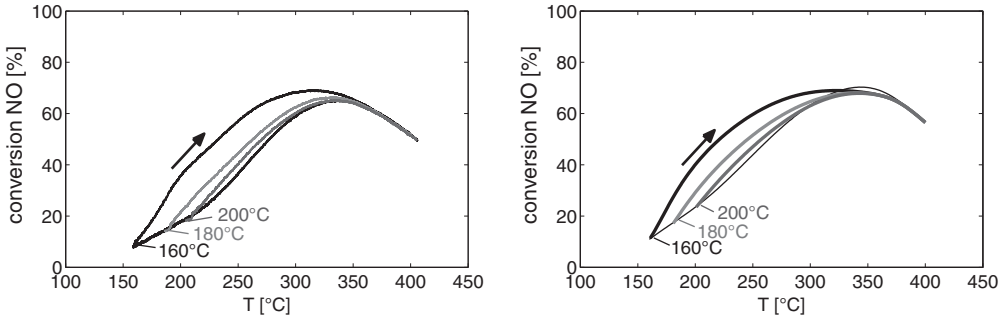

Fig. 6. Variation of minimal temperature for the temperature ramp with 500 ppm NO, 12% O_2 and 10% H_2O in the feed.

is quite close to the optimal value of one. Large condition values (>1000) indicate a bad-posed problem. On the contrary, the condition would equal zero, if one or several parameters have no effect on the simulation.

A singular-value decomposition of the Jacobi-Matrix gives information about correlated parameters. The calculated singular-values are divided by the maximal value. In our case all scaled values are in the range of 2–20. This indicates that 16 essential directions exist. Therefore all 16 parameters have a significant influence and are not correlated. If correlated parameters would exist, the quotients would show a distinct gap between small and big values. Furthermore the t-values of the parameter fit are computed, which are a measure for the significance of the parameter. The t-values of the parameters are in a similar range (Fig. 5), so they all have a comparable influence on the residuum. Only the activation energy of the NO oxidation itself has a slightly higher influence.

In the following, a validation of the model with other experiments is shown.

A variation of the minimal temperature of the ramp is shown in Fig. 6. It can be seen that a reactivation takes only place at temperatures below 250 °C, which is in accordance with the experimental observations. The difference between the activity of the rising and cooling temperature ramp is increasing with lower minimal temperature.

A simulation of the temperature ramp after cooling down in nitrogen is shown in Fig. 7b. The standard experiment with linear temperature ramp between 160 and 400 °C is plotted for comparison with thin lines. The experimental conversion is slightly higher (Fig. 7a), because fresh catalyst slices were used for this experiment and obviously a longterm irreversible deactivation/aging took place as well with the slices used before.

After cooling down in N_2 from 400 °C, the rising temperature ramp has a considerably increased activity in both experiment and simulation. This is due to the fact that a high platinum fraction prevails at 400 °C and cooling down in N_2 conserves the platinum fraction. If the catalyst is cooled down to 300 °C in reaction gas atmosphere and then further in nitrogen, the following, simulated rising temperature ramp has a lower conversion than the standard ramp and hence contradicts the experimental observations. The platinum fraction at 300 °C is probably underestimated in the simulation. This is due to the fact that the thermodynamical equilibrium of $Pt + 0.5\ O_2 \rightleftharpoons PtO$ (Eq. (1)) has been estimated as well.

In another experiment the temperature ramp was interrupted with 1800 s holding time at different temperatures [15]. Holding with oxygen at 180 °C will slightly decrease the platinum fraction. Therefore, the following heating up shows nearly the identical conversion like without holding time, Fig. 8. Holding with NO and without oxygen reveals a significant reactivation of the catalyst. This is in agreement with the experimental observations. Holding with the reaction gas mixture leads to a significantly higher reactivation in the simulation than in the experiment. This can not be avoided with the here used simple model, because a high reactivation velocity is required below 200 °C to reproduce the hysteresis between cooling and heating. The deviation might be caused by using the reaction order according to stoichiometry or the applied model simplifications.

For further validation of the model, the isothermal experiments with 270 or 510 ppm NO_x in the feed presented in [15] are used. Respective results are presented in the next section together with results from catalysts with different Pt dispersion.

3.2. Model extension to catalysts with different Pt dispersion or loading

In this section it will be evaluated, whether the platinum oxidation model can be applied for catalysts with different Pt content

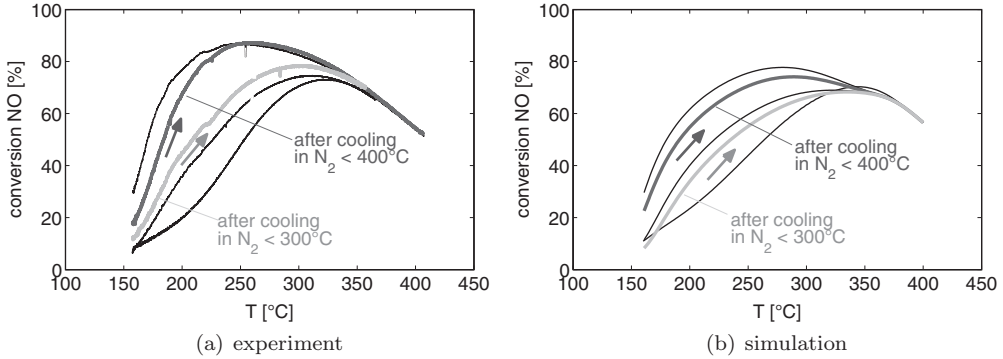

Fig. 7. Experimental (a) and simulated (b) conversion of rising temperature ramp after cooling down in nitrogen from 300 to 400 °C. The standard experiment with linear temperature ramp between 160 and 400 °C is plotted for comparison with thin lines.

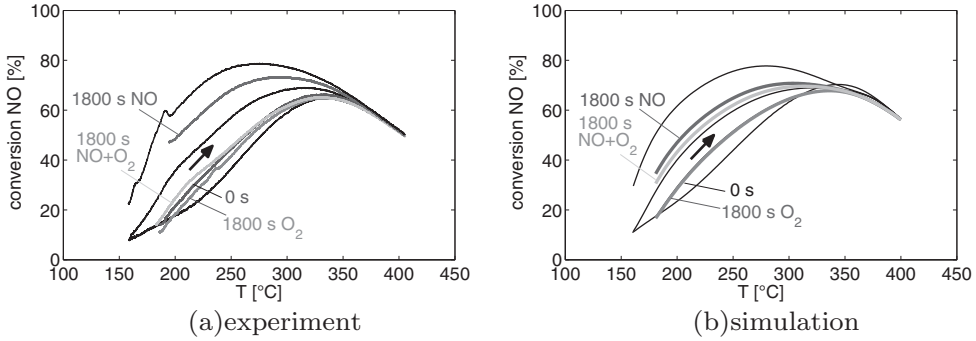

Fig. 8. Experimental (a) and simulated (b) conversion during rising temperature ramp after holding at 180 °C for 1800 s with oxygen or NO or both and 10% H_2O in the feed.

or dispersion. In the following, the so far used catalyst (130.06 g Pt/ft^3-γ-Al_2O_3) is called DOC120. The same catalyst was hydrothermally aged at elevated temperatures (850 and 950 °C) in a furnace for 16 h [20]. These catalysts are referred to as DOC120-850 and DOC120-950. In addition, two catalysts with reduced platinum loading (DOC20: 22.51 g Pt/ft^3, DOC60: 58.37 g Pt/ft^3) were investigated.

Fig. 9 shows that also the temporal progress of platinum oxidation is reproduced quite well with this model for isothermal experiments with 270 ppm NO_x in the feed. For the catalyst DOC120, the model fitted to the temperature ramp was applied without any modification of parameters. For the other catalysts, the measured NO conversion at the beginning and at the end of the isothermal experiment is plotted in Fig. 10 for every 25 K between 150 and 450 °C. The parameters of platinum oxidation and platinum oxide reduction (A_{Pt,O_2}, $A_{PtO,NO}$, E_{Pt,O_2}, $E_{PtO,NO}$) were transferred from DOC120 to the aged and loading reduced catalysts without modification. The parameters (reaction rate constant, activation energy and inhibition term parameters) of the maximal NO oxidation rate r^{Pt}_{NO,O_2} were fitted to the initial conversion of each experiment directly after reducing pretreatment (*start*). For the minimal reaction rate r^{PtO}_{NO,O_2}, it was sufficient to adapt the reaction rate constant to the minimal conversion of each temperature step after 3 h of isothermal NO oxidation (*after 3 h*). The activation energy and inhibition term parameters are kept the same for r^{Pt}_{NO,O_2} and r^{PtO}_{NO,O_2}. This gives a good accordance of simulation and experiment for all modified catalysts, see Fig. 10.

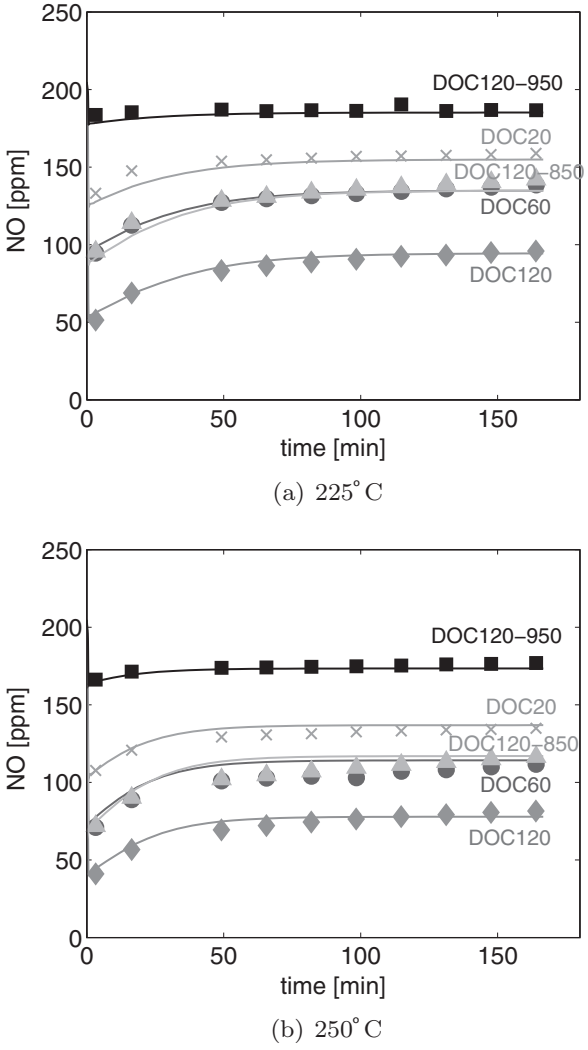

Fig. 9. Temporal progress of deactivation during isothermal experiments after reductive pretreatment (feed: 205 ppm NO, 65 ppm NO_2, 12% O_2, 7% CO_2 and 10% H_2O) at 225 °C (a) and 250 °C (b). Line: simulation. Symbols: experiment.

It can be seen in Fig. 9 that also the temporal progress of NO oxidation is reproduced quite well with these parameters for the aged and platinum loading reduced catalysts. At 225 °C, the accordance is very good. At 250 °C, the experimentally determined deactivation of DOC120, DOC60 und DOC120-850 is slightly lower than in the simulation. But in general, it can be seen that the de- and reactivation parameters can be transferred to other catalysts. A dependency of platinum oxidation on the platinum particle size, as it is repeatedly described in the literature [25,26], is not observed. Otherwise, the aged catalysts, which have substantially larger particle sizes compared to DOC120 [20,28], should show a deviation when using the parameters of DOC120. Such not being the case might be due to the fact that the DOC120 already has quite big particles (>10 nm) and the influence of particle size appears mostly for smaller particles.

A transfer of the platinum oxidation and platinum oxide reduction parameters is hence possible for similar catalyst (Pt/Al_2O_3-DOC) with a different platinum loading or thermal treatment. The extent of deactivation for other washcoat compositions was not investigated. A significant influence is to be expected if platinum is present as an alloy with palladium, as DFT simulations indicate [29], or if the stabilizing component cerium is included in the washcoat [9,24,25,30].

The validation shows that the model fitted only to one temperature ramp experiment is capable to reproduce the most observed phenomena. It is sufficient to include only one additional balance for the platinum oxide fraction and to calculate the NO oxidation on the fast (platinum) and slow sites (platinum oxide) separately. A computation of platinum (and eventually platinum oxide) surface coverages is not necessary. Considering that several assumptions (the actual platinum surface coverage is not calculated in the model, only one reaction for oxide formation and one for reduction is used,

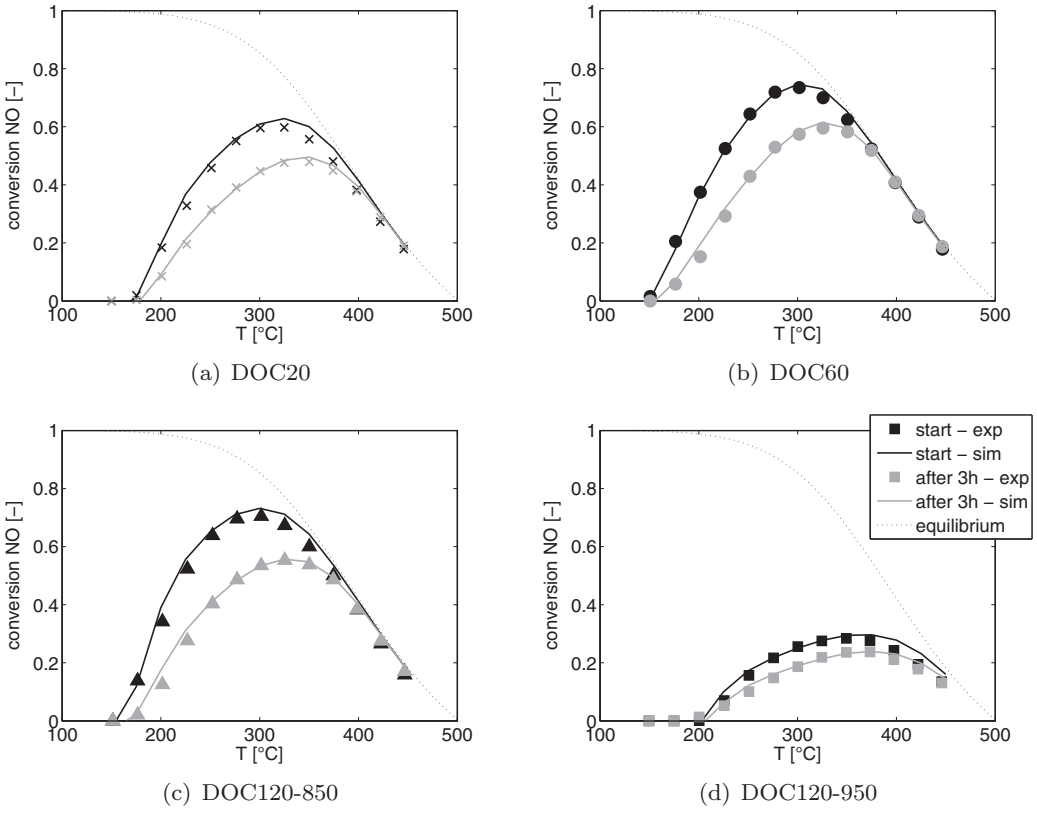

Fig. 10. Conversion of NO oxidation (205 ppm NO, 65 ppm NO_2, 12% O_2, 7% CO_2 and 10% H_2O) on freshly reduced catalysts (*start*) and after 3 h (*after 3h*).

reaction order follows stoichiometry,. . .) are used, certain deviations can obviously not be avoided.

This model does certainly not include all aspects, but it shows the principle approach of how platinum oxidation can be included in a macrokinetic model. In particular, the influence of platinum oxidation on other reactions is so far not taken into account. Experiments with mixtures of CO and NO showed that platinum oxidation also affects the oxidation of other components [5,15]. For a DOC, which is also operated under rich exhaust gas conditions, or a NSC, which is permanently operated in a lean reach cycling mode, the platinum oxide is additionally reduced by reducing agents (H_2, CO, HC) present in the rich exhaust gas. Hence, the activity changes induced by platinum oxidation will be even more pronounced. Due to mutual influences in gas mixtures, the following model compromises so far only the platinum and NO oxidation. The interactions of platinum oxidation with other components (CO, HC, etc.) has to be studied more detailed in the future.

4. Conclusions

Deactivation effects due to platinum oxidation of near series Pt-Al_2O_3 DOC have a substantial influence on the NO oxidation activity. So far, the platinum oxidation and the simultaneous loss of catalyst activity was only accounted for in microkinetic models [5]. In this paper it is shown, that the extension of a macrokinetic model to an additional balance of the platinum fraction and reactions for platinum oxidation ($Pt + 0.5\ O_2 \rightleftharpoons PtO$) and reduction ($PtO + NO \rightarrow Pt + 0.5\ NO_2$) results in a good prediction of platinum oxidation and its influence on the conversion of NO oxidation. The NO oxidation reaction rate is calculated on platinum (higher activity) and platinum oxide (lower activity). The actual NO oxidation rate is computed depending on the platinum fraction. The model is parameterised by only one temperature ramp experiment. Validation simulations show that this model is capable of reproducing the main observed phenomena like reactivation below 250 °C, thermal decay at high temperatures, reactivation while holding times and the temporal progress in isothermal experiments. It is shown that the parameters of de- and reactivation can be transferred to catalysts with a lower platinum loading or aged at higher temperatures, if the NO oxidation on platinum and platinum oxide is reparameterised.

Acknowledgements

The authors would like to gratefully acknowledge the Forschungsvereinigung Verbrennungskraftmaschinen (FVV e.V.) for the financial support and Umicore AG&Co.KG for providing the catalyst.

References

[1] D. Chatterjee, T. Burkhardt, T. Rappe, A. Güthenke, M. Weibel, Numerical Simulation of DOC + DPF + SCR Systems: DOC Influence on SCR Performance, SAE technical papers 01-0867.
[2] R. Marques, P. Darcy, P. Da Costa, H. Mellottée, J. Trichard, Djéga-Mariadassou, Journal of Molecular Catalysis A: Chemical 221 (2004) 127–136.
[3] J. Dawody, M. Skoglundh, E. Fridell, Journal of Molecular Catalysis A: Chemical 209 (2004) 215–225.
[4] L. Olsson, M. Abul-Milh, H. Karlsson, E. Jobson, P. Thormählen, A. Hinz, Topics in Catalysis 30/31 (1) (2004) 85–90.
[5] W. Hauptmann, M. Votsmeier, J. Gieshoff, A. Drochner, H. Vogel, Applied Catalysis B: Environmental 93 (2009) 22–29.
[6] L. Olsson, E. Fridell, Journal of Catalysis 210 (2002) 340–353.
[7] W. Hauptmann, Modellierung von Dieseloxidationskatalysatoren, Ph.D. thesis, Technische Universtität Darmstadt (2009).
[8] H.-F. Wang, Y.-L. Guo, G. Lu, P. Hu, The Journal of Physical Chemistry C 113 (43) (2009) 18746–18752.
[9] J. Després, Adsorption and Catalytic Oxidation of Nitrogen Monoxide in Lean Exhaust for Future Automotive DeNOx Techniques, Ph.D. thesis, Swiss Federal Institute of Technology Zurich (ETH) (2003).
[10] J. Pazmino, J. Miller, S. Mulla, W. Delgass, F. Ribeiro, Journal of Catalysis 282 (1) (2011) 13–24.
[11] J. Segner, W. Vielhaber, G. Ertl, Israel Journal of Chemistry 22 (1982) 375–379.

[12] R. Getman, Y. Xu, W. Schneider, The Journal of Physical Chemistry C 112 (2008) 9559–9572.
[13] R. Getman, W. Schneider, A. Smeltz, W. Delgass, F. Ribeiro, Physical Review Letters 102 (2009), 076101(1-4).
[14] N.A. Saliba, Y.-L. Tsai, C. Panja, B.E. Koel, Surface Science 419 (1999) 79–88.
[15] K. Hauff, U. Tuttlies, G. Eigenberger, U. Nieken, Applied Catalysis B: Environmental 123-124 (2012) 107–116.
[16] C.-B. Wang, C.-T. Yeh, Journal of Catalysis 178 (1998) 450–456.
[17] S. Oh, J. Cavendish, Industrial & Engineering Chemistry Product Research and Development 21 (1982) 29–37.
[18] T. Wang, S. Baek, J.-H. Lee, Industrial & Engineering Chemistry Research 47 (2008) 2528–2537.
[19] Y.-D. Kim, W.-S. Kim, Industrial & Engineering Chemistry Research 48 (2009) 6579–6590.
[20] K. Hauff, U. Tuttlies, G. Eigenberger, U. Nieken, Applied Catalysis B: Environmental 100 (2010) 10–18.
[21] S.B. Kang, H.J. Kwon, I.-S. Nam, Y.I. Song, S.H. Oh, Industrial & Engineering Chemistry Research 50 (9) (2011) 5499–5509. arXiv:http://pubs.acs.org/doi/pdf/10.1021/ie200083f.
[22] M. Wulkow, Macromolecular Reaction Engineering 2 (6) (2008) 461–494.
[23] P. Linstrom, W. Mallard, NIST Chemistry WebBook, NIST Standard Reference Database Number 69, National Institute of Standards and Technology, Gaithersburg, MD (http://webbook.nist.gov/chemistry).
[24] C.-B. Wang, C.-T. Yeh, Applied Catalysis A: General 209 (2001) 1–9.
[25] E. Fridell, A. Amberntsson, L. Olsson, A. Grant, M. Skoglundh, Topics in Catalysis 30/31 (2004) 143–146.
[26] L. Olsson, H. Karlsson, Catalysis Today 147S (2009) S290–S294.
[27] R. Telgmann, Computer aided Modeling Computer- und Softwarekonzepte unterstützen das Modellieren am Beispiel der Technischen Chemie und der Pharmakokinetik, Ph.D. thesis, Freie Universität Berlin (2007).
[28] W. Boll, S. Tischer, O. Deutschmann, Industrial & Engineering Chemistry Research 49 (21) (2010) 10303–10310.
[29] A. Dianat, N. Seriani, M. Bobeth, W. Pompe, L.C. Ciacchi, The Journal of Physical Chemistry C 112 (35) (2008) 13623–13628.
[30] S. Bernard, L. Retailleau, F. Gaillard, P. Vernoux, A. Giroir-Fendler, Applied Catalysis B: Environmental 55 (2005) 11–21.